ChemComm

Accepted Manuscript

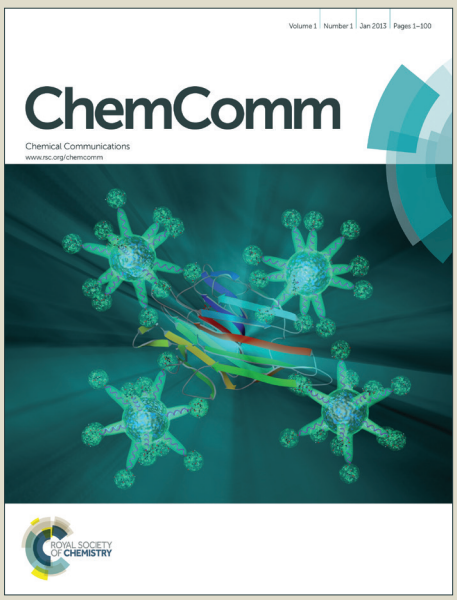

This is an *Accepted Manuscript*, which has been through the Royal Society of Chemistry peer review process and has been accepted for publication.

Accepted Manuscripts are published online shortly after acceptance, before technical editing, formatting and proof reading. Using this free service, authors can make their results available to the community, in citable form, before we publish the edited article. We will replace this *Accepted Manuscript* with the edited and formatted *Advance Article* as soon as it is available.

You can find more information about *Accepted Manuscripts* in the Information for Authors.

Please note that technical editing may introduce minor changes to the text and/or graphics, which may alter content. The journal's standard Terms & Conditions and the Ethical guidelines still apply. In no event shall the Royal Society of Chemistry be held responsible for any errors or omissions in this *Accepted Manuscript* or any consequences arising from the use of any information it contains.

ROYAL SOCIETY OF CHEMISTRY

www.rsc.org/chemcomm

Journal Name

RSCPublishing

COMMUNICATION

In-situ Raman spectroscopic-based microfluidic "lab-on-a-chip" platform for non-destructive and continuous characterization of *Pseudomonas aeruginosa* biofilms

Cite this: DOI: 10.1039/xoxxooooox

Received ooth January 2012,
Accepted ooth January 2012

DOI: 10.1039/xoxxooooox

www.rsc.org/

Jinsong Feng[a], César de la Fuente-Núñez[b], Michael J. Trimble[b], Jie Xu[c], Robert E. W. Hancock[b], Xiaonan Lu[a*]

Pseudomonas aeruginosa **biofilm was cultivated and characterized in a microfluidic "lab-on-a-chip" platform coupled with confocal Raman microscopy in a non-destructive manner. Biofilm formation could be quantified by this label-free platform and correlated well to confocal laser scanning microscopy. This Raman-microfluidic platform could also discriminate biofilms at different developmental stages.**

A biofilm is a consortium of bacteria in which cells associate with each other and adhere to a surface [1, 2]. These sessile cells are embedded within a matrix of secreted extracellular polymeric substances (EPS), including exopolysaccharides, proteins, lipids and nucleic acids, which comprises up to 90% of the biofilm [3]. EPS not only support biofilm structure mechanically, but also encase biofilm bacteria thus allowing them to more easily mediate cell-to-cell communication, and protecting them from environmental stresses, such as antimicrobials [4]. Biofilms on medical devices and food processing surfaces (*e.g.* infusion tubes, water pipes) are highly resistant to antimicrobial treatments and disinfectants and thus represent major health risks [3, 5].

The study of biofilm development is often limited to methods that involve static cultivation conditions, with low shear flow and no nutrient exchange. On the other hand, cultivation under flow conditions more closely mimics biofilms found in the environment and body due to hydrodynamic influences on biofilm structure and cell signalling [6, 7]. For example, biofilm formation of *rpoS*-deficient *Escherichia coli* is impaired under flow cultivation, compared to that under static conditions [8]. The commonly used macro-scale flow cells require large volumes of media, resulting in a relatively expensive system that does not allow for spatial and temporal control of biofilm formation [9]. By precise control of different hydrodynamic conditions, microfluidic platforms can closely simulate the appropriate environmental conditions and allow substantial reductions in reagents used. Microfluidic platforms have been recently applied to the study of bacterial biofilms in a high-throughput manner [10, 11].

However, characterization of biofilms cultivated in a microfluidic platform has been challenging. Most studies have applied confocal laser scanning microscopy (CLSM) for quantitative studies after biofilm staining [12, 13]. However the staining process involved does not allow non-destructive characterization of biofilms in their natural state. Furthermore, chemical variations during biofilm development cannot be fully monitored in a continuous manner. We considered an alternative approach using Raman spectroscopy that can observe vibrational, rotational and other low-frequency energies in a molecule and/or biological system. When coupled with confocal imaging techniques, Raman spectroscopy can be used *in situ* to determine the chemical composition and localization of bacterial biofilms in three dimensions, without staining of bacterial cells [14, 15].

Here, we report the first *in-situ* characterization of *Pseudomonas aeruginosa* biofilms cultivated in a microfluidic platform using confocal micro-Raman spectroscopy in a non-destructive and continuous manner (**Fig. 1**). The microfluidic platform was fabricated by soft lithography (**Fig. S1, ESI†**). The multi-channel microfluidic chip was connected to a pump with bio-compatible tubing. Nutrient broth was continuously infused from the inlet and expelled through the outlet during biofilm formation. Details of *P. aeruginosa* biofilm cultivation in the microfluidic chip are provided in the **ESI†**. The cultivation chamber containing the biofilm was loaded onto a sample stage, which motorized the chip location at a spatial resolution of 2 μm in the horizontal phase and a 3 μm in vertical phase. Confocal Raman microscope was integrated with the microfluidic platform (**ESI†**). Laser introduction and Raman signal collection was conducted through the same 50×

ChemComm Accepted Manuscript

objective. The Raman scattering signal was processed through an aperture, passed through a polarizer, and finally acquired by a CCD detector (**Fig. 1**).

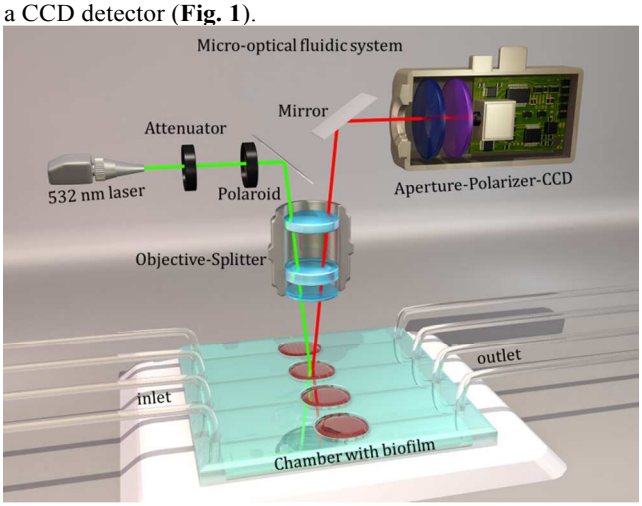

Fig. 1 Schematic illustration of the Raman spectroscopic-based microfluidic "lab-on-a-chip" platform for cultivation and characterization of bacterial biofilms.

To demonstrate the chemical composition of the biofilm, Raman signals from chip substrate (*i.e.* glass slide and polydimethylsiloxane (PDMS) layer) were firstly recorded when the microfluidic chip was filled with medium without inoculation and the focusing state was identical to that subsequently used for biofilm characterization. The chip substrate generated distinct Raman peaks at 485, 610, 703, 785, 860, 1125, and 1402 cm^{-1}. After initial attachment of bacterial cells to the substrate, biofilm started to develop and cover the substrate. The intensity of Raman peaks due to the substrate decreased significantly by 24 h (**Fig. S2, ESI†**). Although biofilm continuously accumulated, the peak intensities from the substrate remained relatively constant, indicating no overlap between biofilm peaks and substrate peaks. Therefore, peaks that were different from substrate peaks and that changed during biofilm development were regarded as deriving from *P. aeruginosa* biofilm.

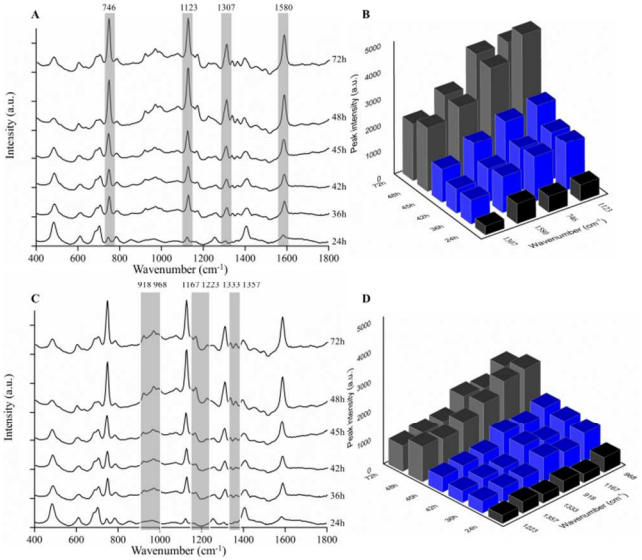

Fig. 2 Raman spectroscopy monitoring of the development of *P. aeruginosa* biofilm in the microfluidic chamber. (A) Prominent peaks appearing within the first 24 h (early stage) are shaded; (B) Variations in intensities of the corresponding Raman peaks (746, 1123, 1307, and 1580 cm^{-1}) over time. (C) Prominent peaks appearing after 48 h (late stage) are shaded; (D) Variations in intensities of the corresponding Raman peaks (918, 968, 1167, 1223, 1333, and 1357 cm^{-1}) over time.

The characteristic Raman peaks for biofilm were averaged and evident in the wavenumber range of 400 to 1800 cm^{-1} in **Fig. 2**. Peaks at 746, 1123, 1307 and 1580 cm^{-1} were prominent and could be clearly observed after 24 h cultivation (**Fig. 2A**). Peaks at 746 and 1580 cm^{-1} were assigned as specific ring structures in nucleic acids (*i.e.* adenine, thymine, guanine), while peaks at 1123 and 1580 cm^{-1} referred to C-C stretching and CH_3/CH_2 twisting or bending respectively which exist widely in carbohydrates, proteins and lipids (**Table S1, ESI†**). The laser (532 nm) used in this study was shown to enhance the Raman signal of cytochrome c by resonance in other organisms [16, 17]. As a highly conserved heme protein, cytochrome c can also be found in *P. aeruginosa.* The prominent peaks at 746, 1123, 1307, and 1580 cm^{-1} showed at similar locations as major bands of pure cytochrome c. Thus, cytochrome c may contribute to Raman spectral pattern of *P. aeruginosa* biofilm. It should be noted that cytochrome c in *P. aeruginosa* is significantly supressed under biofilm conditions [18]. Thus, nucleic acids, proteins, lipids and carbohydrates should still be the major components of biofilm. Irrespective of peak specificity, the increase in Raman peak intensities correlates to biofilm maturation. We defined the first 24 h as the "early stage" of biofilm development. The results demonstrated that nucleic acids, proteins, lipids, carbohydrates, and cytochrome c were synthesized when biofilm started to form. After 36 h cultivation, the intensity of the major early peaks (*i.e.* at 746, 1123, 1307 and 1580 cm^{-1}) increased significantly and then remained relatively constant to 45 h. The significant change that occurred at 36 h could be regarded as a stage switch of biofilm development. Accordingly, we defined 36 h to 45 h as the "mid stage" of biofilm development. The major compositions of biofilm at "mid stage" were almost the same as that of "early stage", but with a higher amount. This indicated that the biofilm had been preliminarily established and synthesis of basic components was temporarily ceased. The intensity of the major early peaks (*i.e.* at 746, 1123, 1307 and 1580 cm^{-1}) increased significantly up to a maximum at 48 h and then remained relatively constant (**Fig. 2B**), indicating that 48 h was another critical time point for a switch in the stage of biofilm development, and the synthesis of basic components in *P. aeruginosa* biofilm did not increase after 48 h. This result indicated that accumulation of basic components into the biofilm was periodic rather than continuous.

P. aeruginosa biofilm also showed Raman peaks at 918, 968, 1167, 1223, 1333, and 1357 cm^{-1} (**Fig. 2**). Peaks at 918, 1167, 1223, and 1333 cm^{-1} were assigned to carbohydrates and proteins, while peaks at 968 and 1357 cm^{-1} were likely due to lipids and nucleic acids (**Table S1, ESI†**). The intensity of these peaks was too weak to be observed until 45 h, but increased substantially from 45 h to 48 h, and then kept relatively constant until 72 h (**Fig. 2C**). After 48 h of cultivation, biofilm was considered to have entered "late stage" development using these peaks as indicators. Compared to the counterpart peaks shown in the spectra of biofilm at 24 h cultivation, peaks at 918, 968, 1167, 1223, 1333, and 1357 cm^{-1} in the spectra of biofilm at 48 h cultivation demonstrated 3.1, 3.2, 6.0, 3.7, 3.5 and 1.7 fold increases in intensity, respectively (**Fig. 2D**). Peaks assigned to proteins and carbohydrates (918, 1167, 1223, and 1333 cm^{-1}) had higher increases than those for nucleic acids (968 and 1357 cm^{-1}), indicating proteins and

ChemComm Accepted Manuscript

This journal is © The Royal Society of Chemistry 2012

carbohydrates accounted for the largest proportion of synthesized substances at this stage. Taken together, we defined biofilm developmental stages according to the appearance of prominent peaks and the significant increases in peak intensity. The results indicated that *P. aeruginosa* biofilm produced different substances at two different stages (*i.e.* early stage and late stage).

To confirm the variations of *P. aeruginosa* biofilms developed at different time points shown in the Raman spectra, principle component analysis (PCA) was utilized. PCA was able to cluster samples on the basis of chemical information and enable further differentiation. **Fig. 3** demonstrates analytical groups for different biofilm samples according to the score plot of principle component 1 (PC1) and component 2 (PC2) from the PCA model. Loading the profiles of PC1 and PC2 accounted for 92.85% and 4.78% of the total variation in spectra, respectively (**Fig. S3, ESI†**). The separating lines, derived from a support vector machine classification algorithm, clearly separated clusters due to biofilms at 24 h, biofilms at 36 h to 45 h, and biofilms at 48 h to 72 h into three groups. The *Mahalanobis* distance between these groups ranged from 5.57 to 12.83. Clusters with interclass distance values higher than 3 are considered to be significantly different ($P < 0.05$) from each other [19]. This result further confirmed the obvious stage switches occurred at 24-36 h (early stage) and 45-48 h (late stage) during biofilm development within the first 72 h (**Fig. 2**). We accordingly defined the biofilm grown between 24 h and 48 h as the "mid stage".

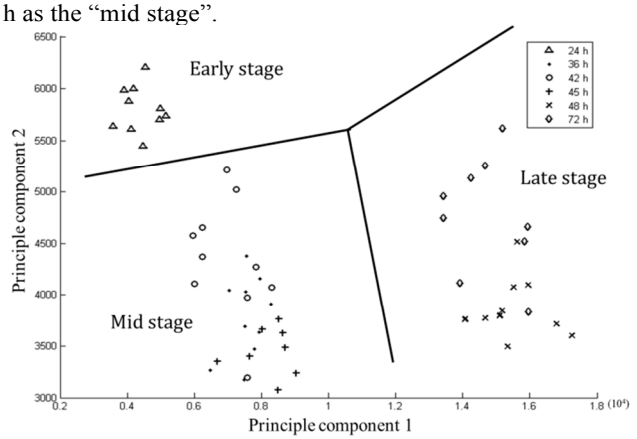

Fig. 3 Representative two-dimensional principle component analysis for the segregation of *P. aeruginosa* biofilms at different development stages. The boundary lines could be used to cluster different groups.

As a parallel study, CLSM was applied to quantify the extent of formation of *P. aeruginosa* biofilm. CLSM uses Cyto-9 dye added at various times to identify biofilm mass and optical sectioning and reconstruction to give a 3D perspective. The amount of biofilm increased as a function of cultivation time (**Fig. 4A**). At 24 h, the biofilm consisted of a thin, nearly confluent layer of bacteria without large structures. At 36 h, the confluent layer had increased more than double in depth. Between 42 and 45 h, the biofilm remained relatively similar to that seen at 36 h, although it must be pointed out that the necessity to stain biofilms for this method means that different biofilms were imaged at each time point. At 48 h, the biofilm increased in thickness and denser microcolonies started to form. Biofilms were very mature after 72 h of growth, which is consistent to the results obtained using a more conventional large volume flow cell apparatus [20]. Based upon CLSM images, the mean biofilm thickness was calculated to quantifiably reflect the physiological changes (**Fig. 4B**). The total height of cultivation chamber in the microfluidic chip was 50 μm. At 24 h, mean biofilm thickness was 5.24 μm. Up to 36 h, it had a 2.4-fold increase to 12.71 μm and remained constant until 45 h. The mean thickness of biofilm reached a maximum of 24.75 μm at 48 h cultivation, which was 1.95-fold greater than that of biofilm at 36 h.

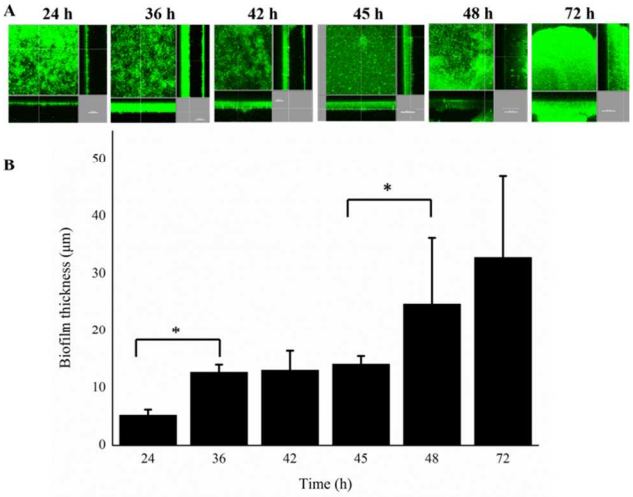

Fig. 4 Representative confocal laser scanning microscopic images of *P. aeruginosa* biofilms grown in a microfluidic chamber. (A) Each panel shows reconstructions from the top in the large panel and sides in the right and bottom panels (xy, yz, and xz dimensions). Biofilm thickness (μm) increased over time. (B) All the values were measured by confocal laser scanning microscopy. Statistical significance was determined using Student's *t*-test (* denotes $P < 0.05$).

Both the Raman and CLSM results demonstrated that the formation of *P. aeruginosa* biofilm increased significantly ($P < 0.05$) after 24 h (end point of the early stage) and 48 h (starting point of the late stage). Therefore, the correlation between the Raman and CLSM results was examined. Partial least squares regression (PLSR) model was constructed (**Fig. 5**). When fitted the calculated biofilm thickness (from Raman spectra) to the measured biofilm thickness (from CLSM) in the PLSR model, these two sets of data showed a close correlation, with a regression coefficient (R-square) of 0.9783. Thus, the PLSR result confirmed that chemical variations (Raman) and physiological variations (CLSM) in *P. aeruginosa* biofilms cultivated in the microfluidic chip occurred concurrently.

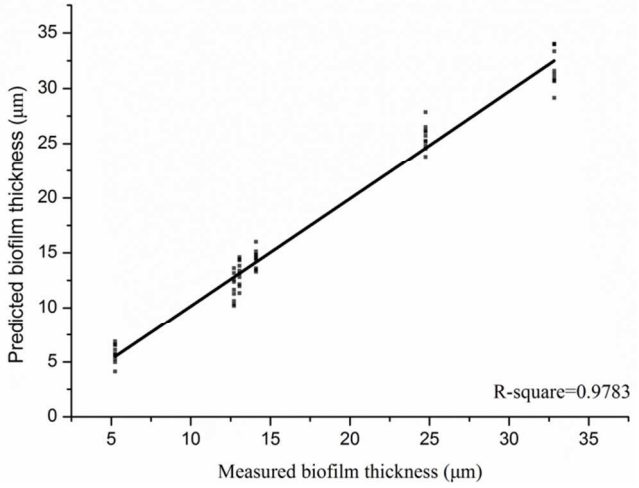

ChemComm Accepted Manuscript

Fig. 5 Correlation of biofilm thickness measured by confocal laser scanning microscopy and calculated by Raman spectroscopy coupled with partial least-squares regression.

According to previous reports, biofilm development has four major stages, including attachment, accumulation, maturation and dispersion [21, 22]. Our current study depicted two important stage switches from attachment to early accumulation (early stage to mid stage) and then to maturation (mid stage to late stage) based on chemical and physiological assessments. However, no evidence was obtained to demonstrate any stage switch from maturation to dispersion. This is most likely due to the fact that dispersion usually occurs at the end of a long period of cultivation, and is induced by environmental stresses (*e.g.* starvation and accumulation of toxic wastes) and regulated by signalling molecules [23, 24]. In the current study, biofilm was developed in a fluidic environment in which nutrients were supplied continuously. In addition, wastes were continuously expelled to reduce the accumulation of toxic substances and signalling molecules. Hence, it is logical to expect a longer maturation time than for static cultivation. Cultivation for 72 h may not be sufficient time to monitor any biofilm switch to the dispersion stage. Another explanation is that accumulation and dispersion within a biofilm might occur simultaneously when the biofilm is fully mature [25]. Hence, the biomass and thickness are in a dynamic balance for a long period, and the maturation and dispersion stages could not be differentiated. A long-term monitoring might be necessary to enable completion of the biofilm dispersion stage. Identification of a specific molecule synthesized at the dispersion stage would provide further evidence for identifying this important stage.

Conclusions

To the best of our knowledge, this study presents a first attempt to develop a non-destructive and label-free *in situ* platform to characterize bacterial biofilms in a precisely controlled hydrodynamic environment. The Raman spectroscopy-based microfluidic "lab-on-a-chip" platform demonstrates the ability to characterize and distinguish *P. aeruginosa* biofilms in different developmental stages (*i.e.* early, mid, and late stages). In addition, Raman results were well correlated with CLSM analyses, demonstrating their feasibility for quantifying biofilm thickness and determining chemical composition simultaneously. Future work is required to apply this platform to screen antimicrobials for the inactivation of biofilms in a high-throughput manner.

Financial support to X.L. in the form of a Discovery Grant from the National Sciences and Engineering Research Council of Canada (NSERC RGPIN-2014-05487) is gratefully acknowledged. R.E.W.H. holds a Canada Research Chair in Health and Genomics and this publication was also supported by the National Institute of Allergy and Infectious Diseases of the National Institutes of Health (NIH) under Award Number R21AI098701 and by a grant from the Canadian Institutes for Health Research MOP-74493. The content is solely the responsibility of the authors and does not necessarily represent the official views of the NIH. C.D.L.F.-N. received a scholarship from the Fundación "la Caixa" and Fundación Canadá (Spain).

Notes and references

[a] Food, Nutrition, and Health Program, Faculty of Land and Food Systems, The University of British Columbia, Vancouver, British Columbia, V6T 1Z4, Canada
[b] Centre for Microbial Diseases and Immunity Research, Department of Microbiology and Immunology, The University of British Columbia, Vancouver, British Columbia, V6T 1Z4, Canada
[c] Department of Mechanical and Industrial Engineering, University of Illinois at Chicago, Chicago, Illinois, 60607, United States.

† Electronic Supplementary Information (ESI) available: Experimental information (materials and methods) and supplementary data (Table S1., Fig S1, S2, S3 and S4). See DOI: 10.1039/c000000x/

1. J. Costerton, P. S. Stewart and E. Greenberg, *Science*, 1999, **284**, 1318-1322.
2. C. de la Fuente-Núñez, F. Reffuveille, L. Fernandez and R. E. Hancock, *Current opinion in microbiology*, 2013, **16**, 580-589.
3. L. Hall-Stoodley, J. W. Costerton and P. Stoodley, *Nature Reviews Microbiology*, 2004, **2**, 95-108.
4. D. Davies, *Nature reviews Drug discovery*, 2003, **2**, 114-122.
5. B. P. Conlon, S. E. Rowe and K. Lewis, in *Biofilm-based Healthcare-associated Infections*, Springer, 2015, pp. 1-9.
6. M. J. Kirisits, J. J. Margolis, B. L. Purevdorj-Gage, B. Vaughan, D. L. Chopp, P. Stoodley and M. R. Parsek, *Journal of Bacteriology*, 2007, **189**, 8357-8360.
7. B. Purevdorj, J. Costerton and P. Stoodley, *Applied and Environmental Microbiology*, 2002, **68**, 4457-4464.
8. A. Ito, T. May, K. Kawata and S. Okabe, *Biotechnology and Bioengineering*, 2008, **99**, 1462-1471.
9. J. S. Webb, L. S. Thompson, S. James, T. Charlton, T. Tolker-Nielsen, B. Koch, M. Givskov and S. Kjelleberg, *Journal of Bacteriology*, 2003, **185**, 4585-4592.
10. J. Kim, M. Hegde, S. H. Kim, T. K. Wood and A. Jayaraman, *Lab on a Chip*, 2012, **12**, 1157-1163.
11. M. R. Benoit, C. G. Conant, C. Ionescu-Zanetti, M. Schwartz and A. Matin, *Applied and Environmental Microbiology*, 2010, **76**, 4136-4142.
12. J. L. Song, K. H. Au, K. T. Huynh and A. I. Packman, *Biotechnology and Bioengineering*, 2014, **111**, 597-607.
13. W. Shumi, J. Lim, S.-W. Nam, K. Lee, S. H. Kim, M.-H. Kim, K.-S. Cho and S. Park, *BioChip Journal*, 2010, **4**, 257-263.
14. N. P. Ivleva, M. Wagner, H. Horn, R. Niessner and C. Haisch, *Analytical and Bioanalytical Chemistry*, 2009, **393**, 197-206.
15. N. P. Ivleva, M. Wagner, H. Horn, R. Niessner and C. Haisch, *Analytical Chemistry*, 2008, **80**, 8538-8544.
16. M. Okada, N. I. Smith, A. F. Palonpon, H. Endo, S. Kawata, M. Sodeoka and K. Fujita, *Proceedings of the National Academy of Sciences*, 2012, **109**, 28-32.
17. D. S. Read, D. J. Woodcock, N. J. Strachan, K. J. Forbes, F. M. Colles, M. C. Maiden, F. Clifton-Hadley, A. Ridley, A. Vidal and J. Rodgers, *Applied and Cnvironmental Microbiology*, 2013, **79**, 965-973.
18. M. Whiteley, M. G. Bangera, R. E. Bumgarner, M. R. Parsek, G. M. Teitzel, S. Lory and E. Greenberg, *Nature*, 2001, **413**, 860-864.
19. X. Lu, Q. Liu, J. A. Benavides-Montano, A. V. Nicola, D. E. Aston, B. A. Rasco and H. C. Aguilar, *Journal of Virology*, 2013, **87**, 3130-3142.
20. C. de la Fuente-Núñez, F. Reffuveille, E. F. Haney, S. K. Straus and R. E. Hancock, *PLoS Pathogens*, 2014, **10**, e1004152.
21. D. Monroe, *PLoS biology*, 2007, **5**, e307.
22. P. S. Stewart and M. J. Franklin, *Nature Reviews Microbiology*, 2008, **6**, 199-210.
23. D. McDougald, S. A. Rice, N. Barraud, P. D. Steinberg and S. Kjelleberg, *Nature Reviews Microbiology*, 2012, **10**, 39-50.
24. T. Bjarnsholt, T. Tolker-Nielsen, N. Høiby and M. Givskov, *Expert Reviews in Molecular Medicine*, 2010, **12**, e11.
25. M. Klausen, M. Gjermansen, J.-U. Kreft and T. Tolker-Nielsen, *FEMS Microbiology Letters*, 2006, **261**, 1-11.

ChemComm Accepted Manuscript

 This journal is © The Royal Society of Chemistry 2012

Graphical abstract

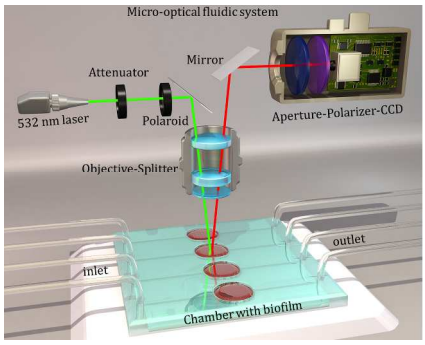

ChemComm Accepted Manuscript